Ultra-Low Dose Amiodarone Reduces Tumor Growth and Angiogenesis

Eliana Steinberg
Hebrew University of Jerusalem Faculty of Medicine
Arnon Fluksman
Hebrew University of Jerusalem Faculty of Medicine
Chalom Zemmour
Hebrew University of Jerusalem Faculty of Medicine
Adi Karsch-Bluman
Hebrew University of Jerusalem Faculty of Medicine
Yifat Brill-Karniely
Hebrew University of Jerusalem Faculty of Medicine
Katerina Tischenko
Hebrew University of Jerusalem Faculty of Medicine
Amy E Birsner
Harvard University
Robert J D'Amato
Harvard University
Ofra Benny (ofrab@ekmd.huji.ac.il)
Hebrew University of Jerusalem Faculty of Medicine

Research

Keywords: Amiodarone, Angiogenesis, Glioblastoma, Ultra-low dose

Posted Date: June 23rd, 2020

DOI: https://doi.org/10.21203/rs.3.rs-37463/v1

Abstract

Background: Pre-clinical studies suggest that Amiodarone induces cytotoxicity in several types of cancer cells, thus making it a potential candidate for use as an anti-cancer treatment. In this study, we examined Amiodarone's effects on glioblastoma multiforme (GBM), a highly aggressive and hypervascularized cancer. We hypothesized that Amiodarone would show an anti-angiogenic effect on GBM in addition to its previously suggested anti-cancer activity, and that an ultra-low dose would be both effective and possibly avert the drug's side effects.

Methods: The anti-cancer activity of Amiodarone was assessed by several in vitro assays using GBM cells. This included cytotoxicity, proliferation, transwell migration, Anoikis, colony-formation and three-dimensional (3D) spheroid growth assays. The anti-angiogenic effect of Amiodarone was tested on endothelial cells, using toxicity, proliferation, migration and tube formation in vitro assays. The anti-cancer and anti-angiogenic activity of Amiodarone was examined in vivo on three different murine models. C57BL/6J mice were utilized for the corneal neovascularization model and the Matrigel plug assay. Foxn1 nu mice were inoculated with GBM cells and used for the GBM tumor xenograft model.

Results: In this study, we showed that Amiodarone has a significant anti-cancer and anti-angiogenic activity in vitro. Moreover, ultra-low dose Amiodarone markedly reduced the size of GBM xenograft tumors and displayed a strong anti-angiogenic effect in vivo.

Conclusions: Our results strongly suggest that Amiodarone possess dual cancer fighting properties.

Background

Amiodarone is a well-known class III anti-arrhythmic drug that has been in clinical use since its introduction into the market more than three decades ago. The drug was approved by the Food and Drug Administration (FDA) in 1985 for the treatment of ventricular tachyarrhythmias and atrial fibrillation. It inhibits various ion channels, including calcium, sodium and potassium channels, making it a potent drug for treating serious anti-arrhythmic cardiac diseases [1–5].

Pre-clinical studies suggest that Amiodarone can reverse multidrug resistance in several types of cancers and enhance cytotoxicity effects both as a single agent or in combination with other anti-cancer drugs [6–9], thus making it a potential candidate for anti-cancer treatment. However, Amiodarone also has an unfavorable toxicity profile affecting a number of organs. Due to its high lipophilicity, Amiodarone accumulates mainly in adipose tissue or highly perfused organs such as the liver, lungs and skin, and its effects may last for months after cessation due to a long biological half-life of up to 100 days [10–12].

The gulf between Amiodarone's anti-cancer potential and its known toxicity profile presents a sizeable challenge to repurposing the drug. In this study, we chose to examine its activity on the aggressive, frequently occurring brain cancer GBM. GBM has a complex biology characterized by uncontrolled proliferation, diffuse infiltration, hypervascularization and resistance to therapies. It is extremely invasive

and angiogenic, characterized by high microvessel density which further contributes to the dreadful prognosis [13–15].

Our aim was to investigate whether Amiodarone also possessed anti-angiogenic properties in addition to its heretofore reported anti-cancer activity. We also wanted to determine whether both these effects continued to occur in doses that were substantially lower than the equivalent standard therapeutic levels for treating cardiac conditions [16].

Data from our in vitro assays, using GBM and endothelial cells, confirmed Amiodarone's strong anti-cancer effects and, for the first time, revealed its significant anti-angiogenic effects. The well-established angiogenesis in vivo models — the Matrigel plug assay and the corneal micropocket assay — showed that ultra-low dose Amiodarone, locally or systemically administered, markedly reduced blood vessel formation in addition to significantly suppressing GBM xenograft tumor growth associated with low tumor vascularization.

We propose that ultra-low dose Amiodarone possesses both anti-cancer and anti-angiogenic activity that should be explored further as a potential candidate for combating highly vascularized tumors.

Materials And Methods

Compliance with Ethical Standards

Mice (C57BL/6J and Foxn1 nu) were purchased from Jackson Laboratories (Bar Harbor, ME, USA). All protocols were approved by the Institutional Animal Care and Use Committee at Children’s Hospital Boston and were conducted in accordance with the Association for Research in Vision and Ophthalmology’s Statement for the Use of Animals in Ophthalmic and Vision Research.

Cell Culture

Human glioblastoma cell line U-87 MG was purchased from ATCC (VA, USA). Human umbilical vein endothelial cells (HUVECs) were obtained from Lonza (Switzerland). All cells were characterized before use, mycoplasma free (using an EZ-PCR Mycoplasma Test Kit (Biological Industries) and used for the experiments up to p15. All cells were kept in a humidified incubator at 37°C with 5% CO_2. For U-87 MG cells EMEM-conditioned medium (Life Technologies, MA, USA) was used and supplemented with 1% L-glutamine, 1% sodium pyruvate, 10% fetal calf serum (FCS) and penicillin/streptomycin. HUVECs were maintained in a specific medium supplemented with PeproGrow-MacroV kit (ENDO-BM & GS-MacroV, PeproTech) and penicillin/streptomycin, and were seeded in wells that were previously coated with gelatin 0.1% (Sigma-Aldrich).

Cytotoxicity Assay with U-87 MG Cells and HUVECs

Each well of the 96-well culture plates (Thermo Fisher Scientific NuNclon^{TM} Delta Surface, Denmark) was seeded with proper medium containing U-87 MG cells (8 000 cells/well) or HUVEC (6 000 cells/well) and

incubated in 37°C and 5% CO_2 for 24 h. Amiodarone (INJ 50 mg/ml, Sanofi-Winthrop, France) was added to each well in varying concentrations (0, 1, 10, and 50 µM with U-87 MG cells, and 0, 0.1, 1, 3, 5, 7 and 10 µM with HUVECs). Stock solution of Amiodarone contains 2% Benzyl alcohol (further diluted), therefore, the proper concentration of benzyl alcohol was added to each treatment. The plate was incubated in 37°C and 5% CO_2 for another 24 h. After incubation, WST-8 reagent (Sigma-Aldrich, Japan) was added into each well for viability detection and incubated in 37 °C and 5% CO_2 for 1 h. Absorbance was measured at 450 nm using a plate reader (Wallac 1420 VICTOR plate-reader, Perkin-Elmer Life Sciences, USA), *n*=10.

Proliferation Assay with U-87 MG Cells and HUVECs

U-87 MG cells (3 000 cells/well) and HUVEC (3 000 cells/well) were incubated for 24 h in their proper conditioned media. Amiodarone in varying concentrations (0, 1, 10, and 50 µM for U-87 MG cells, and 0, 0.1, 1, 3, 5, 7 and 10 µM for HUVECs) was added into all wells. Plates were incubated in 37°C and 5% CO_2 for another 72 h followed by viability detection using WST-8 reagent, *n*=9.

Transwell Migration

U-87 MG cells were harvested and centrifuged for 5 minutes at room temperature (RT). Next, cells were suspended in media containing 1% FCS and counted. For this assay a 24-well cultured plate with 8 µm pore size polycarbonate membrane transwell inserts (Corning Incorporated, USA) was used. Proper medium containing 10% FCS was added to the lower compartments. All inserts were adjusted to allow the membrane to be uniformly submerged in the medium. Next, 1% FCS medium containing 70 000 U-87 MG cells was added to each of the inserts' upper compartments and incubated at 37°C and 5% CO_2 for 30 minutes. After incubation, 1% FCS medium containing different concentrations of Amiodarone (0, 1, 10 and 50 µM) was added to each of the inserts' upper compartments and then incubated at 37°C and 5% CO_2 for 18 h to allow cells to migrate toward the underside of the inserts' filter. After 18 h, cells were fixed, stained and an inverted microscope (OLYMPUS IX73, Japan) was used to detect and count cells on the lower side of the inserts' filter (5 different fields per well) and the average number of migrated cells was calculated, *n*=6.

Anoikis Assay

A pHEMA (Sigma, USA) culture was used to generate Anoikis. A solution containing 20 mg/ml poly(2-hydroxyethyl methacrylate) (pHEMA) in 95% ethanol was prepared and left on a stirrer at RT to dissolve. Once dissolved, the solution was pipetted into 6-well culture plates (Thermo Fisher Scientific NuNclon™ Delta Surface, Denmark). The plates were left in a sterile biological safety cabinet until the ethanol evaporated, and the pHEMA solidified and coated the wells evenly. Proper growth medium containing different concentrations of Amiodarone (0, 1, 10 and 50 µM) was placed in each plate. All plates were seeded with 50 000 U-87 MG cells/well and incubated for 72 h at 37°C and 5% CO_2. After incubation, cell viability was measured using WST-8. Absorbance was measured as previously mentioned, *n*=6.

Soft Agar Assay

Soft agar assay was performed with U-87 MG cells. Six-well culture plates were coated with a bottom layer of 2% agar (Invitrogen by Life Technologies™) and left to solidify in RT. 0.6% agar containing 30 000 U-87 MG cells/well was added to all wells left to solidify in RT. Proper medium containing different concentrations of Amiodarone (0, 1, 5, 7, 10, and 50 µM) was added to all wells. Plates were incubated at 37°C and 5% CO_2. Medium with Amiodarone treatment was refreshed every 5 days. On day 15, colonies were visualized using an inverted microscope (Nikon ECLIPSE TS100). Colonies were fixed, stained and counted (5 different fields per well). Images were processed, and the average number of colonies per well was analyzed and calculated using ImageJ, *n*=3.

Spheroid Growth Assay

15 000 U-87 MG cells/well were seeded in round-bottom 96-well plates (Lipidure®, NY) coated with 2-methacryloyloxyethyl phosphorylcholine (MPC) and treated with varying concentrations of Amiodarone (0, 1, 10 and 50 µM). The plates were incubated at 37°C and 5% CO_2, and images were taken 24 h, 5 and 7 days later using an inverted microscope, as mentioned before. MATLAB code was used to generate the calculated area of the different spheroids, as detailed in the spheroids' image analysis section below, *n*=3.

Spheroid images were cropped to the exact same dimension so that unnecessary background (including pixels of the scale bar) were excluded. Using a MATLAB code, binary B&W images were then formed, in which live spheroids were distinguished from the background (Supplementary fig. 1). The number of pixels was counted in each spheroid. Since individual pictures may be of different resolutions, the total number of pixels in the picture was counted as well and the scaled size of the spheroid was calculated as the ratio between spheroid pixels and the total number of pixels. In some cases, where many dead cells surrounded the live spheroid, the background was cleaned using Photoshop before the B&W image was constructed. In all cases, the scaled spheroids' size was calculated by the ratio between the number of spheroid pixels and the total number of pixels in the cropped image. A further normalization was done in the plots — the spheroid growth was calculated as the ratio between the current size and the initial size, scaling the initial size values of day 1 as 100%.

Scratch Wound Migration Assay

7 000 HUVECs/well were seeded in an IncuCyte® ImageLock 96-well Plate (Sartorius, USA) and incubated in 37°C and 5% CO_2 for 24 h. Varying concentrations of Amiodarone (0, 0.1, 1, 3, 5 and 10 µM) were added to each well and a scratch wound was made in each well using the IncuCyte® 96-well WoundMaker Tool (ESSEN, BioScience). The plate was placed in an incubator containing the IncuCyte® S3 Live-Cell Analysis System (ESSEN, BioScience) for 36 h. Real time automated images were taken every 2 h and cell migration analysis was preformed using the IncuCyte® Scratch Wound Cell Migration Software Module. Final images were processed using ImageJ, *n*=9.

Tube Formation Assay

An endothelial tube formation assay was performed with HUVECs. The wells' bottoms were coated with Matrigel® Matrix (Corning®) 50 µl/well and left to polymerize for 1 h at RT. This was followed by adding 200 µl of Amiodarone in varying concentrations (0, 0.1, 1 and 5 µM) combined with 20 000 cells/well to the Matrigel-coated 96-well plate. The plate was placed in an incubator containing the IncuCyte® S3 Live-Cell Analysis System for 6 h. Real time automated images were taken each hour. Tube formation analysis (calculation of the number of meshes formed) and image processing were done using ImageJ, *n*=4.

Corneal Micropocket Assay

The corneal micropocket assay was carried out as previously detailed [70] in C57BL/6J mice. Micropockets in the mouse cornea were surgically created and pellets containing 80 ng of carrier-free recombinant human basic-fibroblast growth factor (bFGF) (R&D Systems, Minneapolis, MN) were implanted into them. Amiodarone was administered intraperitoneally (I.P.), 0.1 mg/kg/d or 0.05 mg/kg/d q.d. over a course of 5 days. After 5 days, the vascular growth area was measured using a slit lamp and photos of mouse eyes were taken. The area of neovascularization was calculated as vessel area by the product of vessel length measured from the limbus and clock hours around the cornea, using the following equation: vessel area (mm^2) = [clock hours × vessel length (mm) × π × 0.2 mm], *n*=10.

In Vivo Matrigel Plug Angiogenesis Assay

C57BL/6J mice were injected subcutaneously (S.C.) with growth-factor-reduced Matrigel Matrix (BD Biosciences) mixed with recombinant human vascular endothelial growth factor (VEGF) (10 ng/ml) and bFGF (10 ng/ml). Matrigel plugs in the treated groups were additionally mixed with Amiodarone 0.05 mg/plug. After 8 days, Matrigel plugs were removed, embedded in optimal cutting temperature compound (OCT) medium (OCT, Tissue-Teck, USA) and immunohistochemistry was performed using a Vectastain Elite ABC kit (Vector Laboratories) followed by anti-CD31 (BD Biosciences) reaction for micro-vessel staining. Detection was carried out using a 3,3'-Diaminobenzidine chromogen (DAB), resulting in positive brown staining, in addition to using Gill's Hematoxylin for nuclei staining. Quantification of the endothelial cells in Matrigel plugs was performed by Flow cytometry using FACSCalibur and CellQuest software (BD Biosciences, San Jose, CA, USA) following enzymatic digestion of Matrigel plugs, as described elsewhere [71]. Immunostaining was performed for FACS analysis in the presence of rat anti-mouse CD45-APC and CD31+PE (BD Biosciences). Endothelial cells were defined as CD31+CD45- cells, *n*=3.

GBM Tumor Xenograft Model

Foxn1 nu mice were inoculated S.C. with 5×10^6 U-87 MG cells/mouse. Tumor growth was measured transcutaneously with a digital caliper every other day. Tumor volume was calculated using the standard equation: (length × $width^2$ × 0.52). When tumors reached an average volume of ∽200 mm^3, the mice were divided into groups of treated (Amiodarone 0.1 mg/kg or 0.05 mg/kg I.P. injection q.d.) and untreated (given saline) mice over a course of 14 or 24 days, respectively. Tumors were surgically resected and collected when an average volume of ∽1 000 mm^3 was reached. Tumor weight and volume were

measured, followed by embedment in OCT medium and prior to sectioning using a microtome-cryostat. Histological sections were stained using Hematoxylin/Eosin (H&E) or anti-CD31 (DAB) followed by Gill's Hematoxylin, as previously mentioned, n=3-5.

Replications

The *in vitro* experiments were repeated independently at least twice, while the *in vivo* experiments were conducted two times, each with a different dose.

Statistics

Statistical data was analyzed on GraphPad Prism 8 (www.graphpad.com, San Diego, CA). Studies containing two groups were assessed using the unpaired two-tailed Student's *t*-test. Studies containing more than three groups were compared and analyzed using a one-way analysis of variance (ANOVA), and significant differences were detected using Tuckey's multiple comparison post-test. Spheroid radiuses were measured using MATLAB code (as detailed in the Materials and Methods section) and subsequently analyzed by two-way ANOVA. Differences were considered statistically significant for $p < 0.05$.

Results

Amiodarone Affects Viability, Proliferation and Mobility of GBM Cells

Viability assays were carried out on U-87 MG cells, human primary GBM cells, after either 24 or 72 h of incubation with Amiodarone, to investigate cytotoxic and proliferation-rate effects, respectively. Amiodarone induced a mild cytotoxic effect with 50 μM, the highest treatment concentration used in our *in vitro* experiments, reducing the viability of the cells by 28% after 24 h. However, a reduction in the proliferation rate after 72 h already occurred with 10 μM, where 10 and 50 μM treatments led to 18% and 56% reduction, respectively (Fig. 1a). A transwell migration assay was conducted to explore Amiodarone's effect on cell mobility, a pivotal step in cancer progression. In this, cells were seeded in the upper compartment containing 1% FCS and were allowed to migrate to the underside of this higher compartment which contained 10% FCS. After 18 h, migrated cells were counted as presented in Fig. 1b. Doses of 10 and 50 μM of Amiodarone dramatically inhibited cell mobility, with an ∽81% and ∽92% reduction, respectively.

Amiodarone Increases Susceptibility of GBM Cancer Cells to Anoikis

We evaluated Amiodarone's effect on non-adherent cell survival, since GBM is known to be highly metastatic, and non-adherent cell survival in the blood circulation is a crucial factor in metastatic development [17,18]. In this assay, we examined the ability of detached U-87 MG cells treated with Amiodarone to withstand apoptosis for 72 h on a non-adherent surface generated by pHEMA. Fig. 2a shows that control cells had higher survival rates than treated cells: 1 μM and 10 μM significantly reduced cell viability by 34% and 38%, respectively, compared with untreated cells. A marked decrease of 48% in cell viability was detected with 50 μM compared with untreated cells.

Amiodarone Reduces Colony Formation of GBM Cells

There is a correlation between the malignant behavior of tumors and their ability to form colonies in different types of matrixes [19]. In order to investigate whether Amiodarone affects GBM cells' ability to form colonies, we performed a soft agar colony formation assay over 15 days. Fig. 2b, c show Amiodarone's dose-dependent effect on the GBM cells' ability to establish colonies. Cells treated with 5, 7 and 10 μM Amiodarone presented a significant reduction in the number of colonies formed, 23%, 36% and 45%, respectively. Notably, 50 μM of Amiodarone exhibited almost a complete reduction of 92% in the number of colonies formed.

Amiodarone Inhibits GBM Spheroid Growth

Spatial cell-cell interaction and proliferation of U-87 MG cells can be monitored using a 3D spheroid assay which consists of an assembly step and cell growth. Relative spheroid size grown in rounded-bottom 96-well plates under varying concentrations of Amiodarone (0, 1, 10 and 50 μM) was calculated using MATLAB code analysis, as previously shown [20], after 1, 5 and 7 days, as mentioned in the Materials and Methods section (Supplementary fig. 1). Cells under all conditions assembled into spheroids within 24 h of cell seeding (Fig. 2d, e). All control and 1 μM Amiodarone-treated spheroids proliferated and increased in size over time. The control spheroids more than doubled their size after 5–7 days, whereas spheroids treated with 1 μM increased by only ∽40% up to day 7. Spheroids treated with 10 μM Amiodarone preserved their size and did not show further growth. However, 50 μM Amiodarone reduced spheroid size on days 5–7 by ∽30–40%.

Amiodarone Exhibits Anti-Angiogenic Activity In Vitro in HUVECs

Since angiogenesis is a prominent feature of GBM with a strong impact on tumor growth and progression [15,21,22], the functionallity of endothelial cells was investigated. HUVEC viability, mobility and functionality were assessed under Amiodarone treatment. HUVEC cytotoxicity and proliferation assays were measured after 24 and 72 h of drug incubation, respectively. Amiodarone induced cytotoxic effects in all the concentrations used (0.1 – 10 μM) while 10 μM led to a 32% reduction in cell viability. Even the lowest concentration used, 0.1 μM Amiodarone, significantly reduced HUVEC proliferation (Fig. 3a). 0.1, 1 and 3 μM of the drug reduced cell proliferation by 10-18%. A significant dose-dependent effect was observed with higher concentrations of Amiodarone: 5, 7 and 10 μM inducing a reduction of 42%, 57% and 67%, respectively. These results imply that HUVECs are more susceptible to Amiodarone's inhibiting action compared with U-87 MG cells.

The drug's effect on HUVEC mobility was measured in the scratch assay. After 36 h of exposure to the drug, 1 μM Amiodarone-treated cells nearly populated the entire scratch wound area (relative wound density ∽90%), much like the untreated cells shown in Fig. 3b, c. The cells' migration decreased by ∽15% with 5 μM and by ∽30% with 7 and 10 μM.

The tube formation assay predicts the ability of endothelial cells to form stable tubes/branches by mimicking *in vivo* angiogenesis [23]. In this assay, HUVECs treated with 0.1 μM Amiodarone showed no significant effect; however, cells treated with drug concentrations of 1 and 5 μM reduced by ∽40% the number of meshes and branches formed (Fig. 4a, b) compared with untreated cells.

Systemic Amiodarone Treatment Has an Anti-Angiogenic Effect in the Mouse Corneal Neovascularization Model

The mouse corneal micropocket assay using bFGF-induced neovascularization was utilized to evaluate the direct anti-angiogenic activity of Amiodarone following systemic administration in C57BL/6 mice. Amiodarone was administered I.P., 0.05 mg/kg or 0.1 mg/kg q.d., over a course of 5 days. These treatments resulted in a reduction of 22% or 41%, respectively, in the corneal vessel area compared with the control (Fig. 5a, b) with no evidence of side effects. These results indicate a significant inhibition of vessel formation after 5 days of drug treatment.

Amiodarone Decreases Angiogenesis in the Matrigel Plug Assay In Vivo

Amiodarone was locally administered in a quantitative mouse Matrigel angiogenesis assay to investigate its ability to inhibit angiogenesis. Matrigel containing VEGF and bFGF mixed with Amiodarone 0.05 mg/plug was injected S.C. into C57BL/6 mice. On day 8, immunohistochemical staining of blood vessels was performed using anti-CD31 antibodies, enabling visual evaluation of the vasculature in the Matrigel plugs (Fig. 6a). The Matrigel plugs mixed with Amiodarone showed significantly reduced blood vessel formation, as can be visually assessed in Fig. 6a-c. Untreated mice presented bloody plugs surrounded by massive blood vessels with open lumen structures, suggesting functional vessels, compared with Amiodarone-treated mice that showed poor vasculature. Quantification of the infiltrated endothelial cells in Matrigel plugs was accomplished in a single-cell suspension by Fluorescence-Activated Cell Sorting (FACS) (Fig. 6d). Infiltrating endothelial cells were substantially reduced by 60% in the Amiodarone-treated mice group compared with the control group.

Amiodarone Suppresses Tumor Growth and Vasculature of GBM Xenografts

For the *in vivo* anti-tumor activity of Amiodarone, U-87 MG cells were evaluated in S.C. injected Foxn1 nu mice. When the tumors reached an average volume of ∽200 mm^3, the mice were divided into two groups of treated (Amiodarone 0.1 mg/kg q.d. I.P. injection) and untreated mice. After the experiment was terminated, when an average volume of ∽1 000 mm^3 was reached (on day 14), the tumors were surgically resected and collected for histological examination. Significant differences in tumor size and weight between the treated and untreated groups were observed, with average tumor weights of 0.75 gr or 2.36 gr (∽3-fold reduction) and average tumor volumes of 308 mm^3 or 1106.25 mm^3 (>72% reduction), respectively (Fig. 7a-d). Histological H&E staining showed that in addition to reduction in volume, the treated tissues exhibited a more porous and defective structure compared with untreated tumors, possibly due to increased necrosis (Fig. 7e). Immunohistochemical staining of microvessels with anti-CD31 antibodies presented notably lower vascularization compared with untreated tumors (Fig. 7f). Gross

pathology revealed that spleens retrieved from the control group displayed significant splenomegaly compared with the Amiodarone-treated mice (Supplementary fig. 2). With the 0.1 mg/kg q.d. I.P. injection treatment, there were some indications of toxicity in the form of stomach swelling, abnormal liver, and weight loss of up to 14%. Two out of the five mice died on day 10 and 14. One mouse from the control group died on day 14. Reducing the dose to a 0.05 mg/kg q.d. I.P. showed good safety without any significant weight loss while still maintaining effective activity, reducing tumor volume by 40% compared with the control mice on day 24 (Supplementary fig. 3).

Discussion

Amiodarone, a widely administered anti-arrhythmic drug [1], was shown by several pre-clinical studies to reverse multidrug resistance and sensitize several types of cancers to chemotherapy. Pre-clinical studies demonstrated its anti-cancer effects as a single therapeutic or in combination with other anti-cancer drugs on different cancers, including prostate, hepatocellular and breast carcinomas [6–9,24–26]. Based on this, we opted to investigate its anti-cancer effects on GBM, the most common and aggressive primary malignant brain tumor with a dismal prognosis outcome [13]. GBM is a highly vascularized tumor, but in many cases, it shows the potency to invade adjacent and distant areas of the brain in an angiogenesis-independent manner [18,27]. Therefore, finding drugs with dual effects that can target both cancer cells and angiogenesis is of high value. We hypothesized that, in addition to Amiodarone's previously demonstrated anti-cancer effects, it also exhibits prominent anti-angiogenic activity, consequently offering a possible new approach to treating highly vascularized tumors.

The direct effects of Amiodarone on GBM cells were demonstrated in a wide variety of *in vitro* assays using U-87 MG cells. Its most prominent effect was shown to be on cell mobility as demonstrated in the migration assay, where 10 μM of Amiodarone led to a more than 80% inhibition in the number of migrated cells. Proliferation was also reduced with exposure to Amiodarone, but in higher doses (~60% inhibition was obtained with 50 μM).

The observed effect of the drug on cell viability may be related to the induction of cell death as previously shown. Kim et al. demonstrated that Amiodarone induced apoptosis in U-87 MG cells in a dose-dependent manner, and this effect was synergistically enhanced on various malignant glioma cells when combined with tumor necrosis factor (TNF)-related apoptosis-inducing ligand. The associated effect was shown to be mediated by induction of the unfolded protein response (UPR) and an increase of intracellular Ca^{2+} levels, which induced cell death [26]. More recent work demonstrated that the UPR is involved in affecting tumorigenic hallmarks such as cellular metastatic potential and angiogenesis [28,29] and plays an important role in GBM growth and progression [30].

To further investigate Amiodarone's ability to impede the metastatic potential of cancer cells, we measured its effect on the survival of cells in circulation. Anoikis is a programmed cell death activated when cells lose their contact with the extracellular matrix (ECM) occurring during their invasion into the blood circulation. Cancer cells that succeed in evading Anoikis may then colonize in distant organs and

begin the metastatic process [17]. We show that Amiodarone in the range of 1-50 μM, reduced the survival of U-87 MG cells on a non-adherent surface, by ~30-50% (Fig. 2a).

The colonization potential of cancer cells involves an anchorage-independent process requiring cell-cell interactions and proliferation [31]. In our experiments, Amiodarone reduced colony formation and significantly inhibited U-87 MG cells' ability to form aggregates in soft agar in a dose-dependent manner, >90% inhibition. Recently published data by Chang et al. showed a similar trend of Amiodarone's effect on cervical carcinoma cell colonization, suggesting an associated increase in truncated serine and arginine-rich splicing factor 3 (SRSF3), and reduction of RNA (miR)-224. Amiodarone's suppressive effects on the SRSF3 promoter activity were further verified in GBM8401 and U118MG glioma cell lines [6]. Numerous studies demonstrated that SRSF3 and miR-224 are frequently upregulated in glioma cells and are associated with tumor progression and a poor prognosis in glioma patients [32,33].

Similar to colony formation that requires 3D cell interactions, the multicellular spheroid model provides an excellent physiologically relevant model in an ECM-free condition. Unlike monolayer culture, spheroids enable spatial cell-cell interactions and the generation of tissue-like features [20,34]. In the spheroid model, Amiodarone was found to significantly suppress spheroid growth, while 50 μM also induced a notable shrinkage in size. Similar results were reported for patient-derived glioblastoma stem-like cultures showing induction of apoptosis and decreased invasion of tumor neurospheres in association with change in cell cycle and survival gene expression [35]. This is in agreement with other reports demonstrating that Amiodarone inhibited cancer cell migration *in vitro*, and inhibited invasion in a Matrigel assay of human breast cancer cells MDA-MB-231, as well as other murine tumor cells, B16OVA melanoma, JC and 4T-1 breast cancer [24]. Our results point to Amiodarone's potential for reducing tumorigenesis and invasiveness, as demonstrated by the confirmed reduction in motility, invasiveness, proliferation, adherence-free survival and colonization — factors indicative of a tumor's metastatic potential [36].

It is well established that the tumor microenvironment and, more specifically, angiogenesis, have an immense impact on tumor growth [21,22]. Amiodarone's direct effect on endothelial cell function was measured in many *in vitro* assays using HUVECs. We found that HUVECs were more sensitive to Amiodarone compared with U-87 MG cells with respect to viability. Our observations are in agreement with previous studies indicating that Amiodarone may have selective activity, showing relatively nontoxic effects with normal astrocytes while inducing apoptosis in GBM cells [26,35]. In concentrations ranging from 0.1 to 10 μM, Amiodarone significantly reduced cell proliferation (up to ~70%), cell mobility (∽30%) and formation of tubes/branches (∽40%) (Fig. 3, 4). Considering that angiogenesis involves a series of events, including endothelial cell migration, proliferation and tubular formation [37], our *in vitro* results imply that Amiodarone has an anti-angiogenic effect that may be clinically relevant. Moreover, these results, showing tumor angiogenesis suppression, are in line with our results of the *in vivo* angiogenesis model — the Matrigel plug assay [38]. In this animal study, Amiodarone that was mixed into Matrigel plugs (0.05 mg/plug), as a mode of local treatment, extensively reduced the vascularization of the plugs over the course of 8 days. This model provides a direct assessment for endothelial cell recruitment and

their morphogenesis into the blood vessel network. A similar trend was confirmed in the mouse corneal micropocket angiogenesis assay, where Amiodarone, administered systemically over a course of 5 days, induced up to a 40% reduction of vessel formation.

Although angiogenesis is considered to be a hallmark of GBM progression [15,29,30,52], currently the only FDA-approved drug targeting angiogenesis in GBM is the anti-VEGF antibody Bevacizumab [53,54], prescribed for recurrent GBM or as a second-line treatment after standard treatment failure [55]. Several meta-analyses demonstrated that the addition of Bevacizumab to standard therapy improved progression-free survival but failed to improve the overall survival rate. Moreover, there are associated side effects of neurocognitive decline and in health-related quality of life [56–58]. The lack of significant responses to this treatment along with its serious adverse effects emphasizes the advantage of agents with selective and wider action directed against cancer and endothelial cells.

GBM tumor xenografts provide an overall assessment of tumor progression, including both direct processes of cancer cells and indirect anti-cancer tumor microenvironment processes. Amiodarone at the dose of 0.1 mg/kg q.d. I.P., over a course of 14 days, showed over a 70% reduction in tumor volume and weight. Immunohistological staining confirmed an associated reduction in angiogenesis, where untreated tumors showed rich microvessel networks compared with treated mice. The drug's underlying mechanism of action is yet unclear and involves multiple possible target sites, but taken together, our results suggest that Amiodarone possesses anti-angiogenic attributes along with its anti-tumor activity — a dual effect.

One of the key issues with Amiodarone is its adverse side effects when used to treat cardiac dysrhythmias. These include: dangerous polymorphic ventricular arrhythmia due to its blocking potassium channels [39]; dermatologic changes, including photosensitivity and blue-gray skin discoloration [40]; and thyrotoxicosis due to its similarity to thyroxine [10,41]. But the drug's most serious side effect is pulmonary toxicity that can lead to pulmonary fibrosis and death [42]. These clinical symptoms may last months after cessation due to a long biological half-life [12] and may explain the cohort study by Boursi et al., who found that among patients with GBM, active users of Amiodarone for the treatment of their cardiac conditions had a worse survival rate than those who previously had never received the drug [43].

Given this, our study highlights the fact that the anti-cancer activity in the GBM xenograft model can be obtained with an ultra-low dose of Amiodarone compared with the human equivalent dose that is currently prescribed for cardiovascular conditions. The dose of 0.1 mg/kg q.d. I.P. in mice showed some signs of toxicity. However, half of this dose was well tolerated over a course of 24 days, while still inducing a significant reduction in tumor growth. When the same doses of 0.1 mg/kg or 0.05 mg/kg q.d. I.P. were administered for 5 days in the mouse corneal micropocket assays, no side effects were evident, suggesting the possibility of fine tuning the dosage for chronic treatment. Since the pharmacokinetics of substances administered I.P. are similar to those of oral administration [44], it can be concluded that our highest dose administered to mice is equivalent to 0.48 mg/day in a human adult, based on the FDA's guidelines and Reagan-Shaw's conversion formula [45,46]. This is a significantly lower dose than the one

used for treating antiarrhythmic diseases (typically between 100 to 400 mg/day), which is between 200 and 800-fold lower [47].

The positive outcomes using an ultra-low dose, combined with the drug's dual effect, emphasizes Amiodarone's great potential for treating highly vascularized tumors, either systemically or locally.

Conclusions

Taken together, our *in vitro* and *in vivo* results suggest that Amiodarone possesses both significant anti-cancer activity — demonstrated by reduction of tumorigenic processes directly related to tumor progression, such as invasion and colonization — and significant anti-angiogenic activity. We found that ultra-low dose Amiodarone induced tumor shrinkage in GBM xenografts and profoundly reduced blood vessel formation in all mouse models. Repurposing Amiodarone for ultra-low dose systemic or local treatment, in light of its suggested multi-targeting mechanisms, may bypass the drug's negative side effects and become a new standard for cancer treatment. Further study of Amiodarone's underlying cellular mechanisms may also reveal its ability to combat other solid tumors, particularly ones that are largely dependent on angiogenesis.

Abbreviations

GBM: Glioblastoma multiforme; 3D: Three-dimensional; FDA: Food and Drug Administration; HUVEC: Human umbilical vein endothelial cell; FCS: fetal calf serum; RT: Room temperature; pHEMA: poly(2-hydroxyethyl methacrylate); bFGF: basic-fibroblast growth factor; I.P.: Intraperitoneally; S.C.: Subcutaneously; VEGF: Vascular endothelial growth factor; OCT: optimal cutting temperature compound; DAB: 3,3'-Diaminobenzidine chromogen; H&E: Hematoxylin/Eosin; TNF: Tumor necrosis factor; UPR: Unfolded protein response; ECM: Extracellular matrix; SRSF3: serine and arginine-rich splicing factor 3

Declarations

Consent for publication

Not applicable.

Availability of data and materials

All data generated or analyzed during this study are included in this published article and its supplementary information files.

Competing interests

The authors declare that they have no competing interests.

Funding

This study was supported by the Israel Cancer Association (ICA) (No. 0394691), the Israel Foundation of Science (ISF) (No. 0394883) and the Israel Ministry of Science and Technology (MOST) (grant agreement #0394906). The funders had no role in study design, data collection and interpretation, or the decision to submit the work for publication.

Authors' Contributions

Study design: OB and ES; Data collection: ES, AF, CZ, AKB, KT, AEB, RJD and OB; Data analysis: ES, CZ and YBK; Manuscript preparation: ES and OB; Supervision: OB. The authors read and approved the final manuscript.

References

1. Kodama, I.; Kamiya, K.; Toyama, J. Amiodarone: ionic and cellular mechanisms of action of the most promising class III agent. *Am. J. Cardiol.***1999**, *84*, 20R-28R, doi:10.1016/s0002-9149(99)00698-0.
2. Heger, J.J.; Solow, E.B.; Prystowsky, E.N.; Zipes, D.P. Plasma and red blood cell concentrations of amiodarone during chronic therapy. *Am. J. Cardiol.***1984**, *53*, 912–917, doi:10.1016/0002-9149(84)90524-1.
3. Singh, B.N. Amiodarone: Historical development and pharmacologic profile. *Am. Heart J.***1983**, *106*, 788–797, doi:10.1016/0002-8703(83)90002-9.
4. Helmy, I.; Herre, J.M.; Gee, G.; Sharkey, H.; Malone, P.; Sauve, M.J.; Griffin, J.C.; Scheinman, M.M. Use of intravenous amiodarone for emergency treatment of life-threatening ventricular arrhythmias. *J. Am. Coll. Cardiol.***1988**, *12*, 1015–1022, doi:10.1016/0735-1097(88)90470-6.
5. Amiodarone hydrochloride (marketed as Cordarone) information Available online: https://www.fda.gov/drugs/postmarket-drug-safety-information-patients-and-providers/amiodarone-hydrochloride-marketed-cordarone-and-pacerone-information (accessed on May 28, 2020).
6. Chang, Y.L.; Liu, S.T.; Wang, Y.W.; Lin, W.S.; Huang, S.M. Amiodarone promotes cancer cell death through elevated truncated SRSF3 and downregulation of miR-224. *Oncotarget***2018**, *9*, 13390–13406, doi:10.18632/oncotarget.24385.
7. Theodossiou, T.A.; Galanou, M.C.; Paleos, C.M. Novel amiodarone-doxorubicin cocktail liposomes enhance doxorubicin retention and cytotoxicity in du145 human prostate carcinoma cells. *J. Med. Chem.***2008**, *51*, 6067–6074, doi:10.1021/jm800493j.
8. van der Graaf, W.T.A.; de Vries, E.G.E.; Timmer-Bosscha, H.; Meersma, G.J.; Mesander, G.; Vellenga, E.; Mulder, N.H. Effects of Amiodarone, Cyclosporin A, and PSC 833 on the Cytotoxicity of Mitoxantrone, Doxorubicin, and Vincristine in Non-P-glycoprotein Human Small Cell Lung Cancer Cell Lines. *Cancer Res.***1994**, *54*, 5368–5373.
9. Ketchem, C.J.; Kucera, C.; Barve, A.; Beverly, L.J. The Antiarrhythmic Drug, Amiodarone, Decreases AKT Activity and Sensitizes Human Acute Myeloid Leukemia Cells to Apoptosis by ABT-263. *Am. J. Med. Sci.***2018**, *355*, 488–496, doi:10.1016/j.amjms.2018.01.011.

10. Martino, E.; Bartalena, L.; Bogazzi, F.; Braverman, L.E. The Effects of Amiodarone on the Thyroid*. *Endocr. Rev.***2001**, *22*, 240–254, doi:10.1210/edrv.22.2.0427.
11. Basaria, S.; Cooper, D.S. Amiodarone and the thyroid. *Am. J. Med.* 2005, *118*, 706–714.
12. Wiersingal, W.M.; Trip, M.D. *Amiodarone and thyroid hormone metabolism*; 1986; Vol. 62;.
13. Jemal, A.; Siegel, R.; Xu, J.; Ward, E. Cancer Statistics, 2010. *CA. Cancer J. Clin.***2010**, *60*, 277–300, doi:10.3322/caac.20073.
14. Rock, K.; Mcardle, O.; Forde, P.; Dunne, M.; Fitzpatrick, D.; O'neill, B.; Faul, C. A clinical review of treatment outcomes in glioblastoma multiforme-the validation in a non-trial population of the results of a randomised Phase III clinical trial: has a more radical approach improved survival? *Br. J. Radiol.***2012**, *85*, e729–e733, doi:10.1259/bjr/83796755.
15. Louis, D.N.; Ohgaki, H.; Wiestler, O.D.; Cavenee, W.K.; Burger, P.C.; Jouvet, A.; Scheithauer, B.W.; Kleihues, P. The 2007 WHO classification of tumours of the central nervous system. *Acta Neuropathol.* 2007, *114*, 97–109.
16. Hamilton, D.; Nandkeolyar, S.; Lan, H.; Desai, P.; Evans, J.; Hauschild, C.; Choksi, D.; Abudayyeh, I.; Contractor, T.; Hilliard, A. Amiodarone: A Comprehensive Guide for Clinicians. *Am. J. Cardiovasc. Drugs* 2020, 1–10.
17. Tan, K.; Goldstein, D.; Crowe, P.; Yang, J.L. Uncovering a key to the process of metastasis in human cancers: A review of critical regulators of anoikis. *J. Cancer Res. Clin. Oncol.* 2013, *139*, 1795–1805.
18. Lamszus, K.; Kunkel, P.; Westphal, M. Invasion as limitation to anti-angiogenic glioma therapy. *Acta Neurochir. Suppl.* 2003, *88*, 169–177.
19. Saiga, T.; Ohbayashi, T.; Tabuchi, K.; Midorikawa, O. A model for tumorigenicity and metastatic potential: growth in 1.0% agar cultures. *In Vitro Cell. Dev. Biol.***1987**, *23*, 850–4, doi:10.1007/bf02620964.
20. Shoval, H.; Karsch-Bluman, A.; Brill-Karniely, Y.; Stern, T.; Zamir, G.; Hubert, A.; Benny, O. Tumor cells and their crosstalk with endothelial cells in 3D spheroids OPEN. *Sci. Rep.***2017**, *7*, doi:10.1038/s41598-017-10699-y.
21. Yoshida, S.; Ono, M.; Shono, T.; Izumi, H.; Ishibashi, T.; Suzuki, H.; Kuwano, M. Involvement of interleukin-8, vascular endothelial growth factor, and basic fibroblast growth factor in tumor necrosis factor alpha-dependent angiogenesis. *Mol. Cell. Biol.***1997**, *17*, 4015–4023, doi:10.1128/mcb.17.7.4015.
22. Leon, S.P.; Folkerth, R.D.; Black, P.M.L. Microvessel density is a prognostic indicator for patients with astroglial brain tumors. *Cancer***1996**, *77*, 362–372, doi:10.1002/(SICI)1097-0142(19960115)77:2<362::AID-CNCR20>3.0.CO;2-Z.
23. Irvin, M.W.; Zijlstra, A.; Wikswo, J.P.; Pozzi, A. Techniques and assays for the study of angiogenesisa. *Exp Biol Med***2014**, *239*, 1476–1488, doi:10.1177/1535370214529386.
24. Lee, H.C.; Su, M.Y.; Lo, H.C.; Wu, C.C.; Hu, J.R.; Lo, D.M.; Chao, T.Y.; Tsai, H.J.; Dai, M.S. Cancer metastasis and EGFR signaling is suppressed by Amiodarone-induced Versican V2. *Oncotarget***2015**, *6*, 42976–42987, doi:10.18632/oncotarget.5621.

25. Guiu, B.; Colin, C.; Cercueil, J.P.; Loffroy, R.; Guiu, S.; Ferrant, E.; Jouve, J.L.; Bonnetain, F.; Boulin, M.; Ghiringhelli, F.; et al. Pilot study of transarterial chemoembolization with pirarubicin and amiodarone for unresectable hepatocellular carcinoma. *Am. J. Clin. Oncol. Cancer Clin. Trials***2009**, *32*, 238–244, doi:10.1097/COC.0b013e3181845529.
26. Kim, I.Y.; Kang, Y.J.; Yoon, M.J.; Kim, E.H.; Kim, S.U.; Kwon, T.K.; Kim, I.A.; Choi, K.S. Amiodarone sensitizes human glioma cells but not astrocytes to TRAIL-induced apoptosis via CHOP-mediated DR5 upregulation. *Neuro. Oncol.***2011**, *13*, 267–79, doi:10.1093/neuonc/noq195.
27. Sehiffer, D.; Chio, A.; Giordana, M.T.; Mauro, A.; Migheu, A.; Vigliani, M.C. *The vascular response to tumor infiltration in malignant gliomas Morphometric and reconstruction study**; 1989; Vol. 77;.
28. Wang, M.; Kaufman, R.J. The impact of the endoplasmic reticulum protein-folding environment on cancer development. *Nat. Rev. Cancer* 2014, *14*, 581–597.
29. Chevet, E.; Hetz, C.; Samali, A. Endoplasmic reticulum stress–activated cell reprogramming in oncogenesis. *Cancer Discov.* 2015, *5*, 586–597.
30. Peñaranda Fajardo, N.M.; Meijer, C.; Kruyt, F.A.E. The endoplasmic reticulum stress/unfolded protein response in gliomagenesis, tumor progression and as a therapeutic target in glioblastoma. *Biochem. Pharmacol.* 2016, *118*, 1–8.
31. Hamburger, A.W.; Salmon, S.E. Primary bioassay of human tumor stem cells. *Science (80-.).***1977**, *197*, 461–463, doi:10.1126/science.560061.
32. Song, X.; Wan, X.; Huang, T.; Zeng, C.; Sastry, N.; Wu, B.; David James, C.; Horbinski, C.; Nakano, I.; Zhang, W.; et al. SRSF3-regulated RNA alternative splicing promotes glioblastoma tumorigenicity by affecting multiple cellular processes. *Cancer Res.***2019**, *79*, 5288–5301, doi:10.1158/0008-5472.CAN-19-1504.
33. Lu, S.; Wang, S.; Geng, S.; Ma, S.; Liang, Z.; Jiao, B. Upregulation of microRNA-224 confers a poor prognosis in glioma patients. *Clin. Transl. Oncol.***2013**, *15*, 569–574, doi:10.1007/s12094-012-0972-2.
34. Sant, S.; Johnston, P.A. The production of 3D tumor spheroids for cancer drug discovery. *Drug Discov. Today Technol.* 2017, *23*, 27–36.
35. Berghauser Pont, L. *Combination therapies in a patient-derived glioblastoma model*; 2015; ISBN 978-94-91930-38-6.
36. Palmer, T.D.; Ashby, W.J.; Lewis, J.D.; Zijlstra, A. Targeting tumor cell motility to prevent metastasis. *Adv. Drug Deliv. Rev.* 2011, *63*, 568–581.
37. Folkman, J. The role of angiogenesis in tumor growth. *Semin. Cancer Biol.***1992**, *3*, 65–71.
38. Nowak-Sliwinska, P.; Alitalo, K.; Allen, E.; Anisimov, A.; Aplin, A.C.; Auerbach, R.; Augustin, H.G.; Bates, D.O.; van Beijnum, J.R.; Bender, R.H.F. et al Consensus guidelines for the use and interpretation of angiogenesis assays. *Angiogenesis* 2018, *21*, 425–532.
39. Nafrialdi; Kurniawan, T.G.; Setiawati, A.; Makmun, L.H. QT interval prolongation associated with amiodarone use in Cipto Mangunkusumo Hospital, Jakarta. *Acta Med. Indones.***2014**, *46*, 292–7.

40. Enseleit, F.; Wyss, C.A.; Duru, F.; Noll, G.; Ruschitzka, F. The blue man: Amiodarone-induced skin discoloration. *Circulation***2006**, *113*, e63, doi:10.1161/CIRCULATIONAHA.105.554303.
41. Jonckheer, M.H. Amiodarone and the thyroid gland. A review. *Acta Cardiol.***1981**, *36*, 199–205.
42. Wolkove, N.; Baltzan, M.; Frcp, M.D. *Amiodarone pulmonary toxicity*; 2009; Vol. 16;.
43. Boursi, B.; Han, H.J.; Haynes, K.; Mamtani, R.; Yang, Y.X. Ion channel blockers and glioblastoma risk and outcome: a nested case–control and retrospective cohort studies. *Pharmacoepidemiol. Drug Saf.***2016**, *25*, 1179–1185, doi:10.1002/pds.4054.
44. Turner, P. V.; Brabb, T.; Pekow, C.; Vasbinder, M.A. Administration of substances to laboratory animals: Routes of administration and factors to consider. *J. Am. Assoc. Lab. Anim. Sci.* 2011, *50*, 600–613.
45. Center for Drug Evaluation and Research *Estimating the Maximum Safe Starting Dose in Initial Clinical Trials for Therapeutics in Adult Healthy Volunteers*; 2005;
46. Reagan-Shaw, S.; Nihal, M.; Ahmad, N. Dose translation from animal to human studies revisited. *FASEB J.***2008**, *22*, 659–661, doi:10.1096/fj.07-9574lsf.
47. Mahmarian, J.J.; Smart, F.W.; Moyé, L.A.; Young, J.B.; Francis, M.J.; Kingry, C.L.; Verani, M.S.; Pratt, C.M. Exploring the minimal dose of amiodarone with antiarrhythmic and hemodynamic activity. *Am. J. Cardiol.***1994**, *74*, 681–686, doi:10.1016/0002-9149(94)90309-3.

Figures

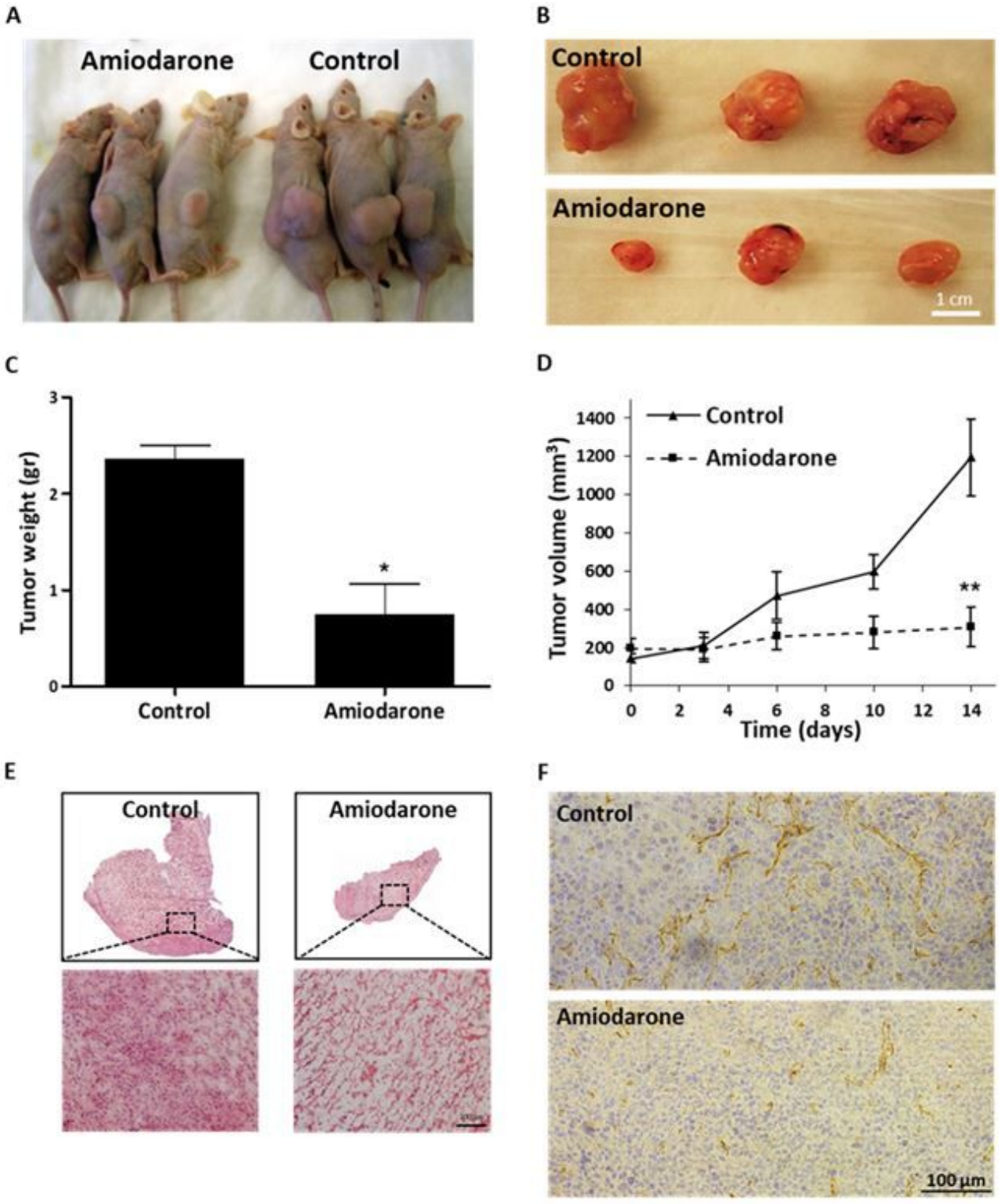

Figure 1

Amiodarone inhibits GBM tumor xenograft growth. Amiodarone's anti-tumor activity following systemic administration (I.P.) evaluated in a S.C. tumor model. Foxn1 nu mice were inoculated S.C. with 5 x 106 U-87 MG cells. When tumors reached an average volume of ~200 mm3, mice were divided into two groups of treated (Amiodarone 0.1 mg/kg I.P. injection q.d.) and untreated (given saline) mice over a course of 14 days. a, b Tumors were surgically resected and collected when an average volume of ~1000 mm3 (day

14) was reached. c, d Weight and volume of tumors from treated and untreated mice were measured. Tumor volume was calculated using the standard equation (length × width2 × 0.52). n=3-5. *p<0.05, **p<0.01, compared with non-treated control mice. Results are presented as mean ± SEM. e Representative histologic sections of untreated tumor (left) and Amiodarone-treated tumor (right) of mice post-H&E staining. Scale bar: 100 μm. f Representative images of tumor sections stained with anti-CD31 (DAB- brown) and Gill's Hematoxylin for nuclei staining (blue). Untreated tumor (top) and Amiodarone-treated tumor (bottom). Scale bar: 100 μm. Objective lens 10x.

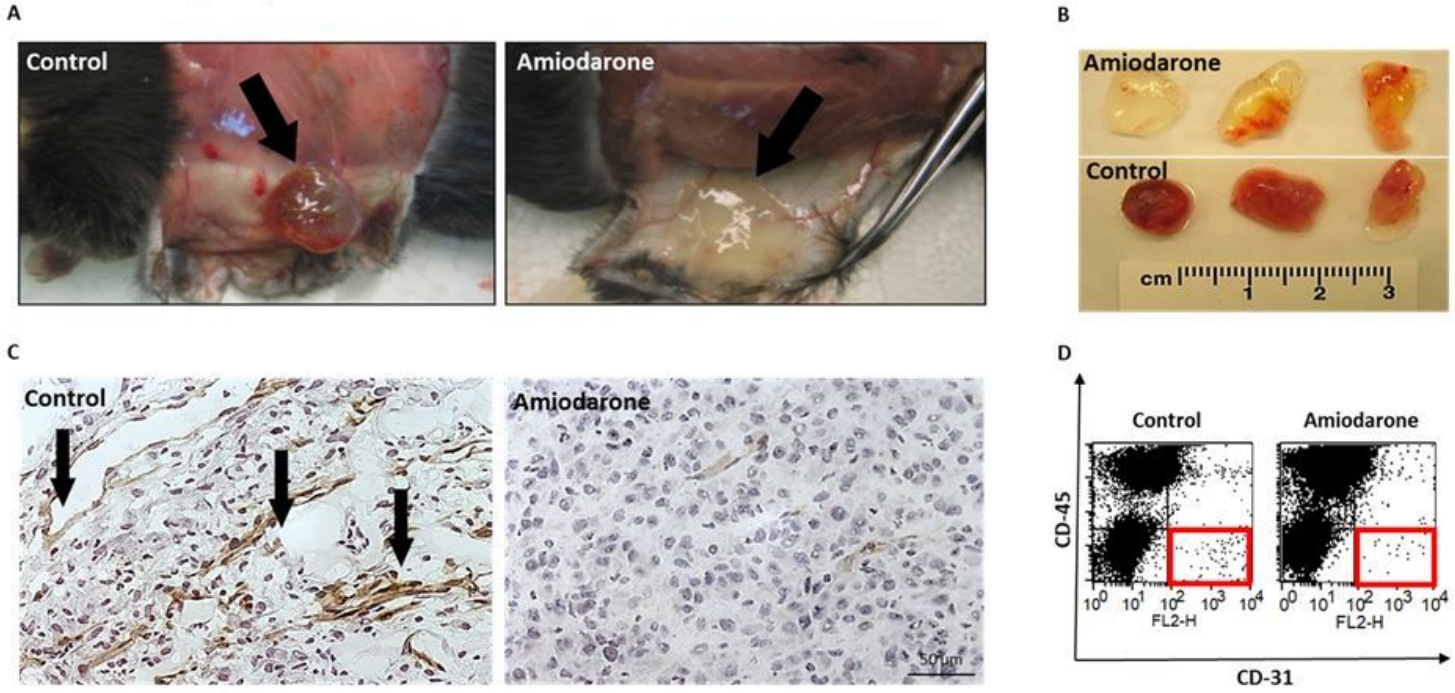

Figure 2

Amiodarone inhibits angiogenesis in Matrigel plugs. Matrigel containing VEGF and bFGF (control) or Matrigel containing VEGF and bFGF mixed with Amiodarone 0.05 mg/plug was injected S.C. into C57BL/6 mice to determine the drug's effect on angiogenesis. a, b Representative plugs removed from Amiodarone-treated and untreated mice after 8 days. Untreated mice presented bloody plugs surrounded by massive blood vessels, compared with Amiodarone-treated mice which had poor vasculature. c Representative histologic sections of untreated plug (left) and Amiodarone-treated plug (right) of mice post anti-CD31 antibody (DAB-brown) and Gill's Hematoxylin for nuclei (blue) staining. Arrows point to large vessels with open lumens. Scale bar: 50 μm. d Quantification of infiltrating endothelial cells in Matrigel plugs employing the Flow cytometry assay. FACS dot plots of endothelial cells (CD31+/CD45, marked in red squares) from single-cell suspension originated from untreated (left) and treated (right) Matrigel plugs. Data are presented as percent of specific cell population out of the total cell population (p<0.05). Infiltrating endothelial cells were reduced by 60% in the Amiodarone-treated mice group compared with the non-treated control group. n=3. Objective lens 400x.

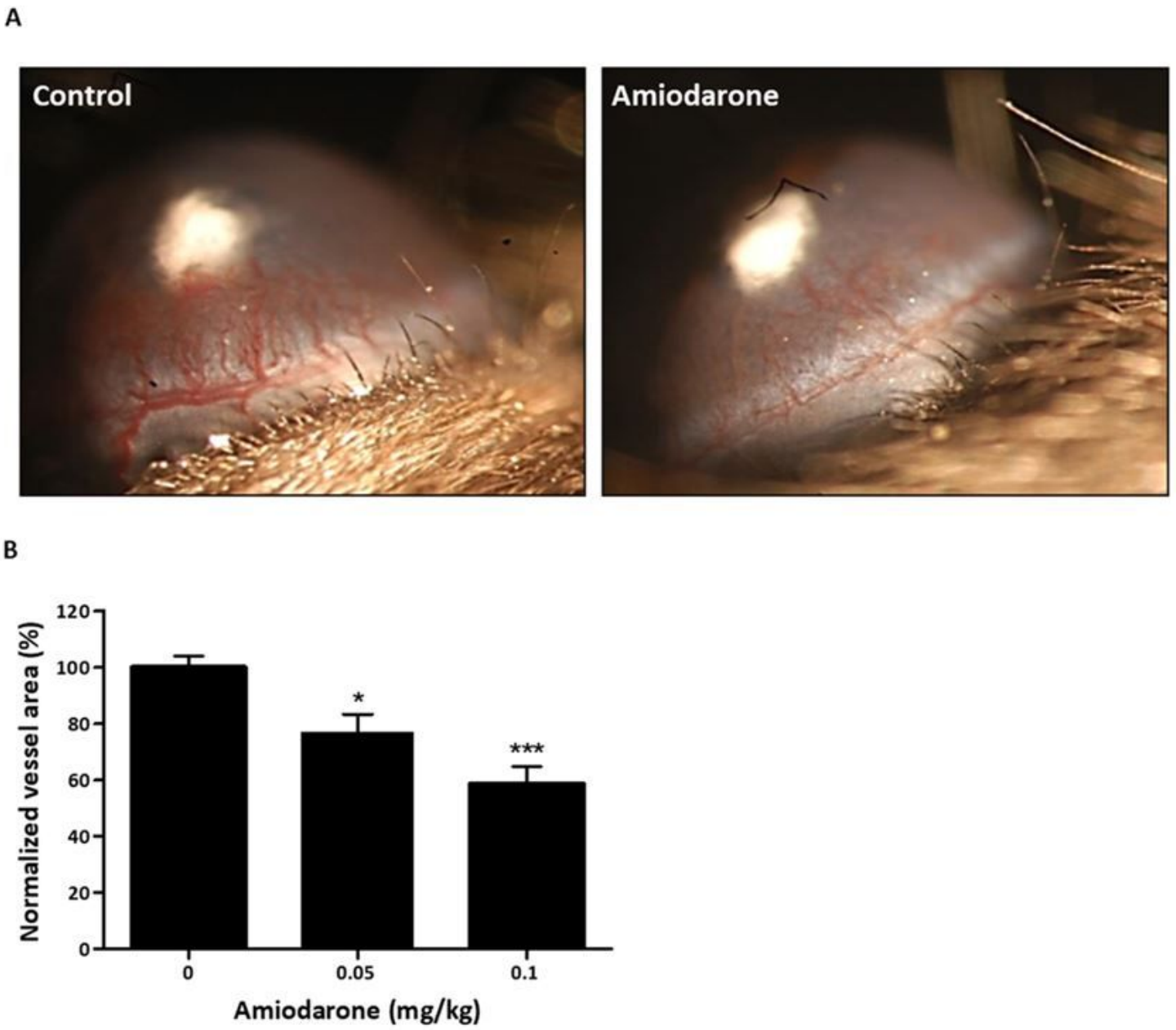

Figure 3

Amiodarone inhibits corneal neovascularization after I.P. treatment. Amiodarone's anti-angiogenic activity evaluated following systemic administration in the mouse corneal micropocket assay using bFGF-induced neovascularization. C57BL/6 mice were injected I.P. with Amiodarone 0.05 mg/kg or 0.1 mg/kg q.d. for 5 days. a Representative images taken from treated (0.1 mg/kg q.d.) and untreated mice on day 5. bFGF pellets detected as a white spot in the center of the cornea. Blood vessels growing from limbal periphery are reduced in the Amiodarone-treated group compared with the untreated group. b Normalization of vessel area (%) for untreated and Amiodarone treated mice (0.05 mg/kg and 0.1 mg/kg q.d.). Vessel area was calculated using the following formula: [Clock hours × Vessel length (mm) × π × 0.2 mm]. Graphs indicate significant inhibition of vessel formation after 5 days of treatment. Objective

lens 400x, (in each group n=10). *p<0.05, ***p<0.001, compared with non-treated control mice. Results are presented as mean ± SEM.

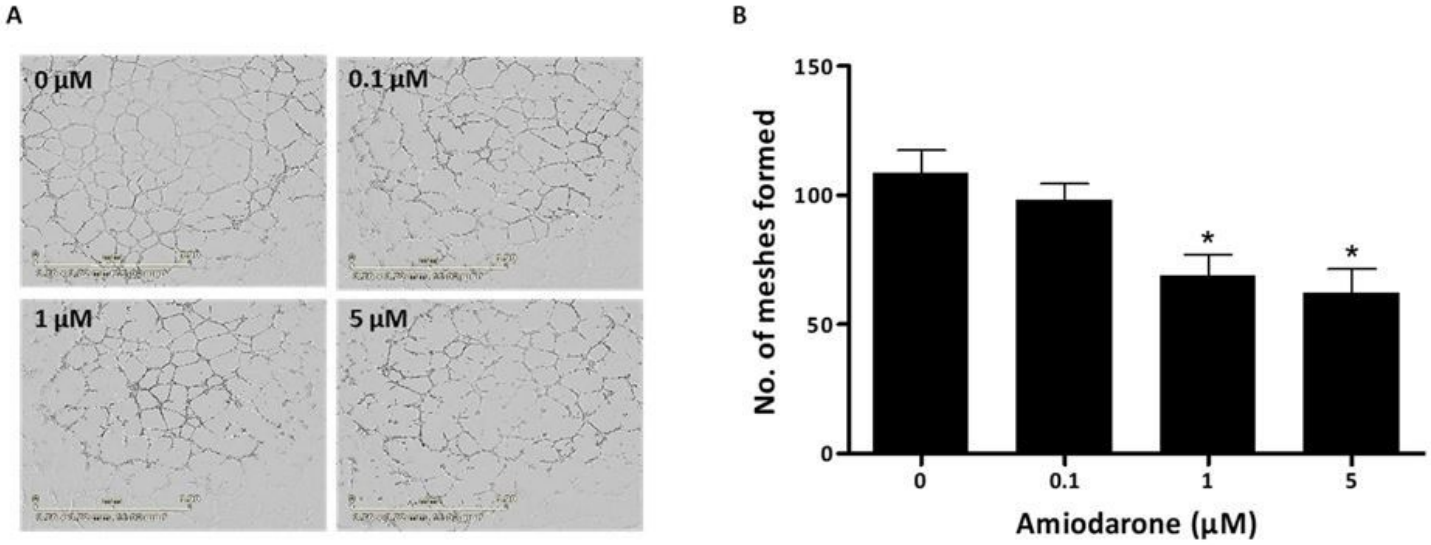

Figure 4

Amiodarone affects HUVEC function in 3D. a, b Angiogenesis tube formation assay of HUVECs seeded on Matrigel® after 6 hours of incubation, using IncuCyte® S3 Live-Cell Analysis System with ranging concentrations of Amiodarone (0, 0.1, 1 and 5 µM). Statistical analysis of tube formation hallmark (number of meshes formed) and images processed using ImageJ software; representative images are presented, n=4. Scale bar: 1.9 mm. *p<0.05, compared with non-treated control cells. Results are presented as mean ± SEM.

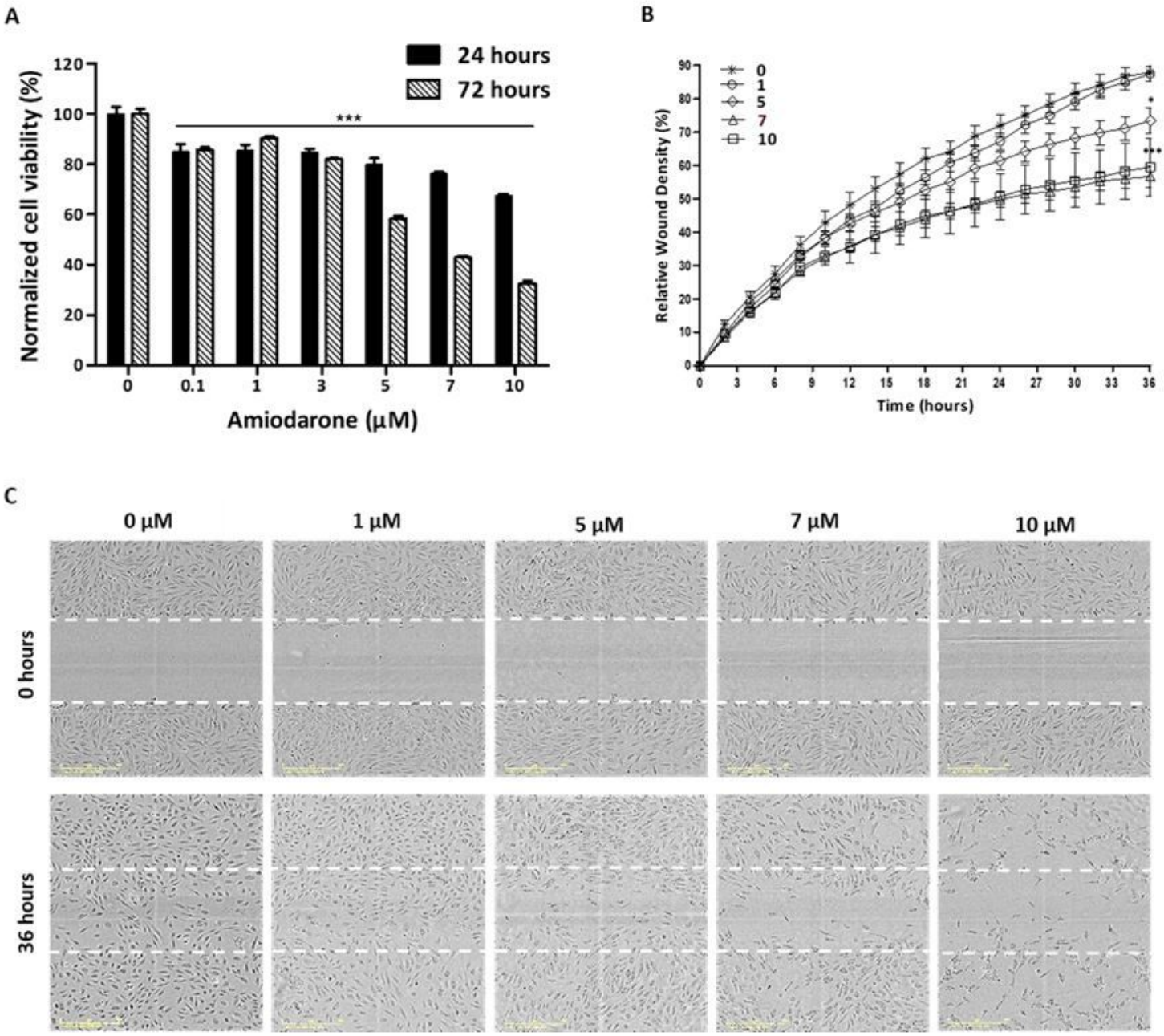

Figure 5

Amiodarone affects HUVEC function. a Viability assay of HUVECs, using WST8, after 24 and 72 hours of incubation with ranging concentrations of Amiodarone (0, 0.1, 1, 3, 5, 7, and 10 µM), investigating cytotoxic and proliferation-rate effects, respectively, n=8. ***p<0.001, compared with untreated cells with the same incubation time. b, c Scratch assay of HUVECs after 36 hours of incubation using the IncuCyte® S3 Live-Cell Analysis System, with ranging concentrations of Amiodarone (0, 1, 5, 7, and 10 µM), n=8. Scale bar: 400 µm. *p<0.05, ***p<0.001, compared with non-treated control cells. Thin white dashed lines present the scratch area. Results are presented as mean ± SEM.

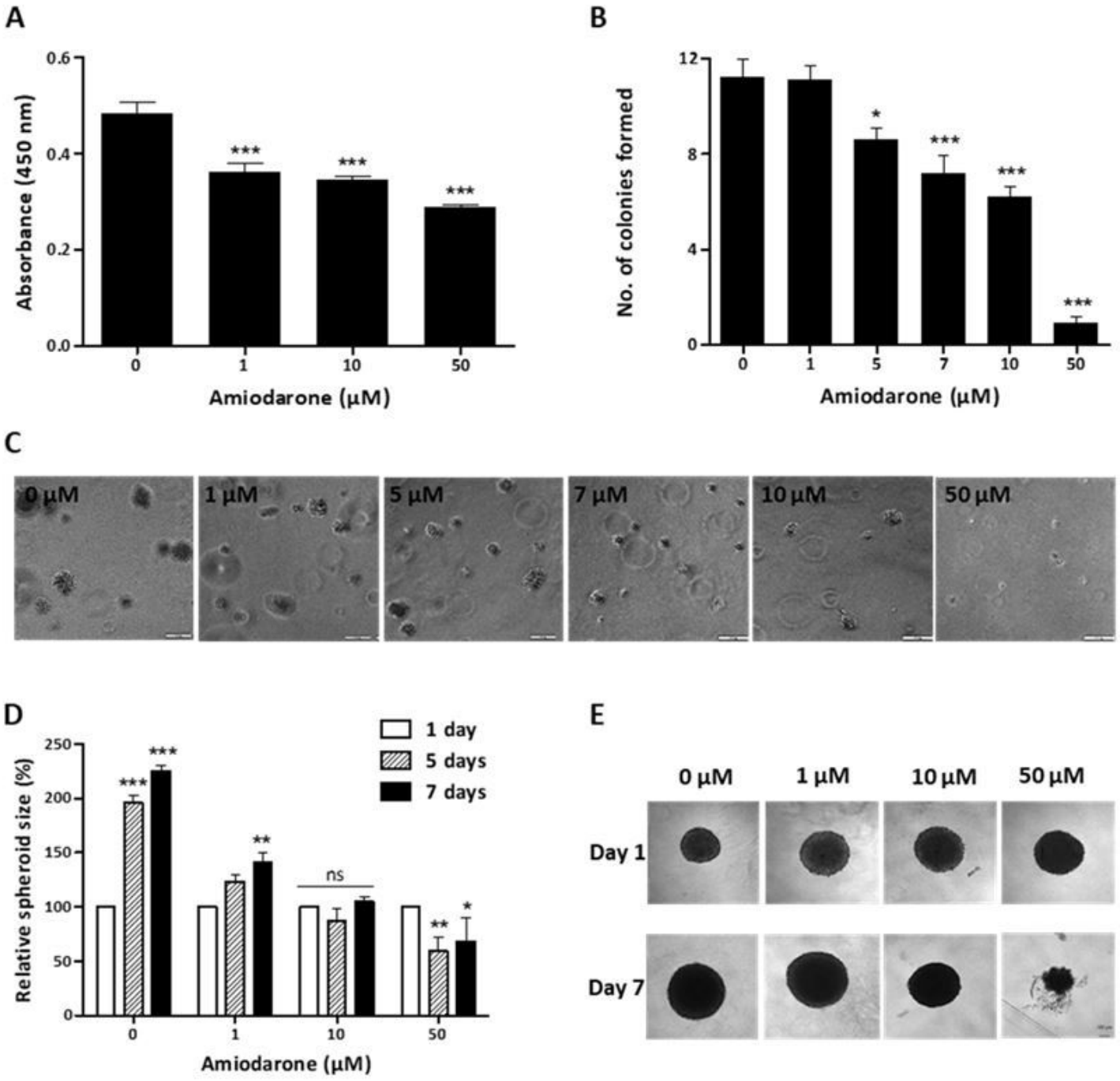

Figure 6

Amiodarone affects U-87 MG cell function in 3D. a Anoikis assay with U87-MG cells, using p-HEMA coated plates, incubated with ranging concentrations of Amiodarone (0, 1, 10 and 50 μM) for 72 hours. Cell viability measured using WST8 assay, n=6. ***p<0.001, compared with non-treated control cells. b, c Soft agar colony formation assay of U-87 MG cells cultured for 15 days under ranging concentrations of Amiodarone (0, 1, 5, 7, 10, and 50 μM). Colonies visualized using inverted microscope on day 15. Images processed, analyzed, then average number of colonies per well using ImageJ calculated. n=3. *p<0.05, ***p<0.001, compared with non-treated control cells. Scale bar: 100 μm. d, e Spheroid assembly and growth assay of U-87 MG cell spheroids. Relative spheroid size grown in rounded-bottom 96-well plate

after 1, 5 and 7 days under ranging concentrations of Amiodarone (0, 1, 10 and 50 μM). Calculated using MATLAB code analysis. Further normalization done in the plots - spheroid growth calculated as the ratio between the current size and the initial size, scaling the initial size values of day 1 as 100%, n=3. *p<0.05, **p<0.01, ***p<0.001, ns, not significant. Results are presented as mean ± SEM. Scale bar: 100 μm.

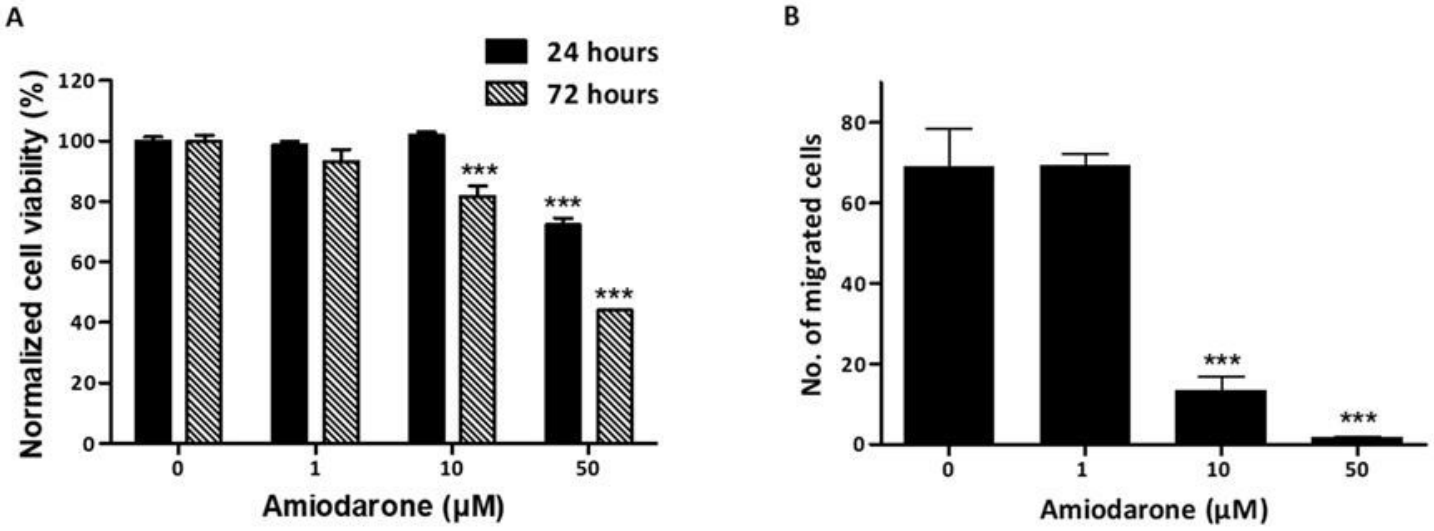

Figure 7

Amiodarone affects U-87 MG cell function. a Viability assay of U-87 MG cells using WST8, after 24 or 72 hours of incubation with ranging concentrations of Amiodarone (0, 1, 10 and 50 μM), investigating cytotoxic and proliferation-rate effects, respectively. n=9-10. ***p<0.001, compared with non-treated control cells with the same incubation time. b Transwell migration assay of U-87 MG cells after 18 hours of incubation with ranging concentrations of Amiodarone (0, 1, 10, and 50 μM). Inverted microscope used to detect and count cells on the lower side of inserts' filter (five different fields per well) and average number of migrated cells calculated, n=6. ***p<0.001, compared with non-treated control cells. Results are presented as mean ± SEM.

Supplementary Files

This is a list of supplementary files associated with this preprint. Click to download.

- Supplementary21.6.2020.docx
- Supplementary21.6.2020.docx